A Novel Head-to-Head Conformer of d(GpG) Cross-linked by Pt: New Light on the Conformation of Such Cross-links Formed by Pt Anticancer Drugs

Susan O. Ano,[†] Francesco P. Intini,[‡] Giovanni Natile,*[,‡] and Luigi G. Marzilli*[,†]

Contribution from the Department of Chemistry, Emory University, Atlanta, Georgia 30322, and Dipartimento Farmaco-Chimico, Università degli Studi di Bari, 70125 Bari, Italy

Received February 19, 1998. Revised Manuscript Received August 6, 1998

Abstract: The critical DNA lesion accounting for the anticancer activity of *cis*-$PtCl_2(NH_3)_2$ and its analogues [*cis*-PtX_2A_2: A_2 = a diamine or two amines, X_2 = anionic leaving ligand(s)] is an unusual intrastrand *cis*-Pt(d(GpG))A_2 cross-link with Pt linking N7's of adjacent guanines (G). The only known cross-link form with two anti G's, HH1, has head-to-head (HH) bases. We provide NMR, HPLC, and mass spectral evidence for a second, distinct HH *cis*-Pt(d(GpG))A_2 cross-link conformer, HH2, in **Bip**Pt(d(GpG)) (**Bip** = 2,2′-bipiperidine, where the coordinated **Bip** has *R*, *S*, *S*, and *R* configurations at the asymmetric N, C, C, and N chelate ring atoms). The HH1 and HH2 **Bip**Pt(d(GpG)) conformers are formed both kinetically and thermodynamically in comparable amounts. The NMR results showed for both **Bip**Pt(d(GpG)) conformers that the bases were *anti*, *anti* HH, the 5′-G sugar pucker was N, and the 3′-G sugar pucker was S. The major difference between the HH1 and HH2 conformers is the propagation direction of the phosphodiester linkage. Molecular modeling calculations with NMR restraints on the HH1 and HH2 conformers indicate comparable energies and no unusual features that should have precluded prediction of the existence of the HH2 conformer. Calculations led to similar conclusions for the *cis*-Pt(d(GpG))$(NH_3)_2$ HH2 conformer. During the two decades of intense interest in this cross-link, this new form has gone unrecognized, although published results have suggested the presence of unknown conformers. Our results in this first report of a second *anti*, *anti* HH d(GpG) adduct place an entirely different perspective on the conformational diversity of *cis*-Pt(d(GpG))$(NH_3)_2$ in solution. Although the new HH2 conformation is unlikely to exist in a duplex at low temperature, the new form may be important in mutational events, in duplex breathing, or in duplex interactions with DNA damage recognition proteins and repair enzymes. Finally, the spectral features, especially the H8 NMR signals, of HH1 d(GpG) species in single strands and in duplexes are typically very different, results attributed to differences in both extent and direction of base canting. **Bip** is an example of a chirality controlling chelate (**CCC**) ligand that can influence canting. The HH1 conformer of **Bip**Pt(d(GpG)) is the first single-stranded species that has key spectral characteristics very similar to those of a typical duplex cross-linked species. Thus, even the HH1 conformer of **Bip**Pt(d(GpG)) is an unusual species.

Introduction

The exceptional anticancer activity displayed by cisplatin (*cis*-$PtCl_2(NH_3)_2$) and its analogues [*cis*-PtX_2A_2: A_2 = a diamine or two amines, X_2 = anionic leaving ligand(s)][1] is usually attributed to a unique type of intrastrand d(GpG) lesion with Pt cross-linking N7's of adjacent anti G's of DNA.[2] In both single-stranded and duplex adducts, the cross-link is widely believed to adopt an *anti*, *anti* head-to-head (HH) conformation with N and S puckers for the 5′ and 3′ sugars, respectively.[1,3−11] This *anti*, *anti* conformer, called HH1 here, has two recognized variants with different directions of base canting. Typically, the 5′-G base cants toward the 3′-G, and the 3′-G base cants toward the 5′-G in single- and double-stranded HH d(GpG) adducts, respectively.[4,5,9,10,12−14] Virtually all reports on both

[†] Emory University.
[‡] Università degli Studi di Bari.

(1) Bloemink, M. J.; Reedijk, J. In *Metal Ions in Biological Systems;* Sigel, H. Sigel, A., Eds.; Marcel Dekker: New York, 1996; Vol. 32, pp 641−685.
(2) Fichtinger-Schepman, A. M. J.; van Oosterom, A. T.; Lohman, P. H. M.; Berends, F. *Cancer Res.* **1987**, *47*, 3000−3004.
(3) Girault, J.-P.; Chottard, G.; Lallemand, J.-Y.; Chottard, J.-C. *Biochemistry* **1982**, *21*, 1352−1356.
(4) den Hartog, J. H. J.; Altona, C.; Chottard, J.-C.; Girault, J.-P.; Lallemand, J.-Y.; de Leeuw, F. A. A. M.; Marcelis, A. T. M.; Reedijk, J. *Nucleic Acids Res.* **1982**, *10*, 4715−4730.
(5) den Hartog, J. H. J.; Altona, C.; van der Marel, G. A.; Reedijk, J. *Eur. J. Biochem.* **1985**, *147*, 371−379.
(6) van der Veer, J. L.; van der Marel, G. A.; van den Elst, H.; Reedijk, J. *Inorg. Chem.* **1987**, *26*, 2272−2275.
(7) Fouts, C. S.; Marzilli, L. G.; Byrd, R. A.; Summers, M. F.; Zon, G.; Shinozuka, K. *Inorg. Chem.* **1988**, *27*, 366−376.
(8) Iwamoto, M.; Mukundan, S., Jr.; Marzilli, L. G. *J. Am. Chem. Soc.* **1994**, *116*, 6238−6244.
(9) Kline, T. P.; Marzilli, L. G.; Live, D.; Zon, G. *J. Am. Chem. Soc.* **1989**, *111*, 7057−7068.
(10) den Hartog, J. H. J.; Altona, C.; van Boom, J. H.; van der Marel, G. A.; Haasnoot, C. A. G.; Reedijk, J. *J. Biomol. Struct. Dyn.* **1985**, *2*, 1137−1155.
(11) Kozelka, J.; Fouchet, M. H.; Chottard, J.-C. *Eur. J. Biochem.* **1992**, *205*, 895−906.
(12) Mukundan, S., Jr.; Xu, Y.; Zon, G.; Marzilli, L. G. *J. Am. Chem. Soc.* **1991**, *113*, 3021−3027.
(13) Herman, F.; Kozelka, J.; Stoven, V.; Guittet, E.; Girault, J.-P.; Huynh-Dinh, T.; Igolen, J.; Lallemand, J.-Y.; Chottard, J.-C. *Eur. J. Biochem.* **1990**, *194*, 119−133.
(14) Yang, D.; van Boom, S. S. G. E.; Reedijk, J.; van Boom, J. H.; Wang, A. H.-J. *Biochemistry* **1995**, *34*, 12912−12920.

10.1021/ja9805674 CCC: $15.00
Published on Web 11/06/1998

single-stranded and duplex adducts indicate that the HH1 conformer predominates, but many reports contain speculation that HH1 equilibrates with other forms that interconvert too rapidly for separate characterization by NMR spectroscopy.[4,9,12,15−17] Recently, two forms were found for a duplex adduct, even when the duplex is bound to an HMG protein.[15,16] One form, with spectral characteristics somewhat similar to those of the platinated single-stranded precursor, has broad NMR signals, suggestive of multiple conformations. In both recent and earlier studies, the nature of alternative d(GpG) cross-link forms was not explicitly determined, and distinct, resolved, multiple forms of simple single-strand GG cross-links are not known.[15,16] The only well-defined alternative d(GpG) cross-link adduct has an HH conformation but with a *syn* G and is found in a hairpin with unusual properties.[8]

Conformers with distinctly different relationships of the d(GpG) to the Pt moiety or of the bases to each other, such as head-to-tail (HT) forms requiring 180° base rotations, have been considered to be either unlikely or highly unfavored. It has generally been thought that the backbone linkage between the bases has two interrelated effects: (i) it makes such rotation very slow or very unfavorable and (ii) it stabilizes the HH1 form. The assumption has been implicit that if HT forms were present the dynamic processes leading to the HH1 form would be slow and the HT form would be detected. Counter-arguments can be raised, however. We note that since the symmetry of a DNA chain is low and each atom is unique, NMR methods cannot easily distinguish the case of one conformer in a relatively fixed state from the case of a mixture of conformers in rapid dynamic motion. Indeed, simple models with unconnected nucleotides are more amenable to NMR study, and these are highly fluxional, interconverting rapidly between forms in which the bases rotate through ∼180°.[18] Adducts with the *cis*-$Pt(NH_3)_2$ moiety itself are especially difficult to elucidate. Attachment of the NH_3 ligands to Pt by single bonds allows the ligands to adopt independently numerous orientations that allow the NH groups to form hydrogen bonds to the nucleic acid target or to avoid steric interactions with the target. As a result, multiple similar conformations probably coexist, and the barriers between the conformers are probably shallow, making *cis*-$Pt(NH_3)_2$ adducts especially fluxional.

We now demonstrate that a single-stranded *cis*-Pt(d(GpG))-A_2 cross-link adduct can exist in multiple conformations in slow exchange. One conformer has the HH1 structure but is unique in having spectral characteristics very similar to those of a duplex adduct. We provide compelling evidence for a novel, distinctly unprecedented *cis*-Pt(d(GpG))A_2 conformer. We show that this new conformer, HH2, also has two *anti* G's and HH bases. As depicted schematically (Figure 1), the main difference between the new HH2 conformer and the accepted HH1 conformer is the direction of propagation of the backbone. During the two decades of intense interest in such unusual and important cross-links, this new conformer has gone unrecognized.

We discovered the HH2 conformer as one of the two main kinetic products from the reaction of d(GpG) with [(*R*,*S*,*S*,*R*)-**Bip**$Pt(H_2O)_2]^{2+}$ (Chart 1). **Bip** (2,2′-bipiperidine) is an example

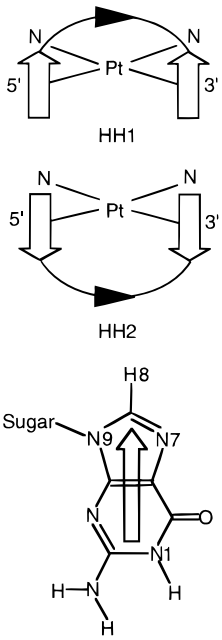

Figure 1. G orientations possible in **Bip**Pt(d(GpG)) adducts. In the scheme, the G coordination sites are forward and the **Bip** ligand is to the rear and mostly omitted for clarity. The open arrows represent the G bases (as shown at bottom), and the small arrows represent the propagation direction of the phosphodiester linkage.

Chart 1

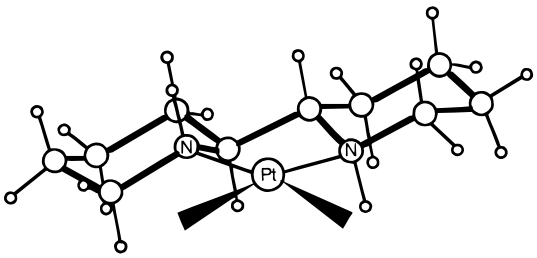

of a chirality controlling chelate (**CCC**) ligand.[19] Because of the dynamic nature of typical Pt cross-linked d(GpG) adducts, we began several years ago to design **CCC** ligands which could both slow the dynamic motions and favor particular conformers in solution.[19−22] Through continued improvements in **CCC** ligand design, we now have available very useful cisplatin analogues with Pt coordinated to **Bip**,[22] a ligand having two favored C_2-symmetrical geometries with (*R*,*S*,*S*,*R*) or (*S*,*R*,*R*,*S*) configurations at the asymmetric N, C, C, and N chelate ring atoms.[22] The NH's of **Bip** are contained in a piperidine ligand ring in addition to the Pt chelate ring, making **Bip** resistant to base-catalyzed inversion of N chirality. The bulk of the **Bip** ligand is concentrated in the Pt coordination plane, a feature designed to slow dynamic processes after product formation. This design was validated in a study of **Bip**Pt(5′-GMP)$_2$ complexes.[22] We thus expected that the adducts formed by [**Bip**$Pt(H_2O)_2]^{2+}$ with oligonucleotides would not be fluxional, and we anticipated that studies on the adducts would provide rewarding insight into the nature of both the kinetic and the

(15) Berners-Price, S. J.; Corazza, A.; Guo, Z.; Barnham, K. J.; Sadler, P. J.; Ohyama, Y.; Leng, M.; Locker, D. *Eur. J. Biochem.* **1997**, *243*, 782−791.
(16) Berners-Price, S. J.; Barnham, K. J.; Frey, U.; Sadler, P. J. *Chem. Eur. J.* **1996**, *2*, 1283−1291.
(17) van Boom, S. S. G. E.; Yang, D.; Reedijk, J.; van der Marel, G. A.; Wang, A. H.-J. *J. Biomol. Struct. Dyn.* **1996**, *13*, 989−998.
(18) Cramer, R.; Dahlstrom, P. *Inorg. Chem.* **1985**, *24*, 3420−3424.
(19) Marzilli, L. G.; Intini, F. P.; Kiser, D.; Wong, H. C.; Ano, S. O.; Marzilli, P. A.; Natile, G. *Inorg. Chem.* **1998**, accepted for publication.
(20) Xu, Y.; Natile, G.; Intini, F. P.; Marzilli, L. G. *J. Am. Chem. Soc.* **1990**, *112*, 8177−8179.
(21) Kiser, D.; Intini, F. P.; Xu, Y.; Natile, G.; Marzilli, L. G. *Inorg. Chem.* **1994**, *33*, 4149−4158.
(22) Ano, S. O.; Intini, F. P.; Natile, G.; Marzilli, L. G. *J. Am. Chem. Soc.* **1997**, *119*, 8570−8571.

thermodynamic products. Indeed, our studies of (*R*,*S*,*S*,*R*)-**Bip**Pt(d(GpG)) (hereafter **Bip**Pt(d(GpG))) reveal novel conformers with unusual properties.

Experimental Section

Materials. Deoxyguanyl(3′-5′)deoxyguanosine (d(GpG)) from Sigma was used as received. The platinum compounds were of the form (*R*,*S*,*S*,*R*)-**Bip**Pt$(NO_3)_2$. The free bipiperidine ligands were prepared by hydrogenation of bipyridine.[23] The purity of the isomers was checked by HPLC by using a RR-DACH DNB column.

Bip$PtCl_2$ complexes were prepared by the substitution of **Bip** for $(DMSO)_2$ in *cis*-Pt$(DMSO)_2Cl_2$. In a typical experiment, a suspension of *cis*-Pt$(DMSO)_2Cl_2$ in methanol (0.42 g, 1 mmol, in 90 mL) was treated with a solution containing a stoichiometric amount of **Bip** (1 mmol of *S*,*S* isomer) in the same solvent (10 mL). After a few hours of stirring, the suspension became a colorless solution and was left overnight. The yellow precipitate formed was collected, washed with water, and dried in vacuo; yield, 80%. The compound proved to be **Bip**$PtCl_2$ as a single isomer ((*R*,*S*,*S*,*R*)-**Bip**$PtCl_2$ for *S*,*S*-**Bip**). Anal. Calcd for $C_{10}H_{20}Cl_2N_2Pt$: C, 27.7; H, 4.6; N, 6.4. Found for (*R*,*S*,*S*,*R*)-**Bip**$PtCl_2$: C, 28.1; H, 4.7; N, 6.3.

The nitrate salts were obtained from the reaction of **Bip**$PtCl_2$ with $AgNO_3$. In a typical experiment, **Bip**$PtCl_2$ (1 mmol) was suspended in acetone (150 mL) and treated with the stoichiometric amount of $AgNO_3$ (2 mmol dissolved in 5 mL of water). After being stirred at room temperature in the dark for 6 h, the suspension was filtered on Celite, and the clear solution evaporated to dryness. The NO_3 salt was obtained in nearly quantitative yield as a white powder. Anal. Calcd for $C_{10}H_{20}N_4O_6Pt$: C, 24.6; H, 4.1; N, 11.5. Found for (*R*,*S*,*S*,*R*)-**Bip**Pt$(NO_3)_2$: C, 25.1; H, 4.3; N, 11.7.

Methods. In a typical in situ preparation, d(GpG) (1 equiv) was treated with (*R*,*S*,*S*,*R*)-**Bip**Pt$(NO_3)_2$ (1 equiv, ~3−5 mM) in D_2O (0.5−1.0 mL) at pH 3.5 and 0 °C; dilute (0.8 mM) conditions were sometimes employed. Reactions were monitored by ^{1}H NMR spectroscopy until no free d(GpG) signal or no change in H8 signal intensity was observed. Samples were eventually lyophilized and redissolved in 99.96% D_2O for 2D NMR experiments.

NMR spectra were obtained on a GE GN600 Omega spectrometer or a Varian Unity+600 and referenced to the residual HOD peak (^{1}H),[24] 3-(trimethylsilyl)tetradeuterosodium propionate (^{1}H and ^{13}C), and trimethyl phosphate (^{31}P). The saturation transfer experiments used a 16K block size and presaturation pulse sequence with a 500 ms delay. Procedures for 2D NMR data acquisition and processing (described in the Supporting Information) included the following: phase sensitive nuclear Overhauser enhancement (NOESY),[25] double-quantum filtered correlation (DQF COSY),[26] ^{1}H−^{31}P reverse chemical shift correlation (RCSC),[27] and gradient ^{1}H−^{13}C heteronuclear single quantum coherence (HSQC) spectroscopy.[28]

Molecular mechanics and dynamics (MMD) calculations using restraints from NMR data were performed using the Discover module of the InsightII 97.0 package (MSI) on a Silicon Graphics Indy workstation. The force field was recently developed in this laboratory.[29] Charges on the **Bip** ligand were determined using the CFF91 force field and corrected for the positive charge from Pt as described elsewhere.[29] The volume integrals of NOE cross-peaks from each conformer, measured with Felix, were normalized to a G H2′-2″ (1.78 Å) NOE cross-peak of that conformer. A 20 kcal/mol force constant was used for the NOE restraints. Minimization typically included 1000 cycles of steepest descents and 5000 cycles of conjugate gradient until a Δ rms gradient of 0.0001 kcal/(mol•Å) was obtained. Dynamics runs were preceded by minimization and consisted of a 500-ps constant temperature simulation at 300 K. The conformers were sampled every 1 ps, and the resulting 500 structures were minimized to a Δ rms gradient of 0.001 kcal/(mol•Å). For both minimization and dynamics calculations, the distance-dependent dielectric constant was set to $4r_{ij}$, while 1−4 nonbonded interactions were scaled by a factor of 0.5.

HPLC separations were performed on a RP-18 (5 μm) column. Eluent A was ammonium acetate (0.02 M) buffer, pH 5.5, and eluent B was ammonium acetate (0.02 M) in 2:1 methanol:H_2O. The gradient employed was 95% A to 15% A over 60 min with a flow rate of 0.7 mL/min. The detection wavelength was 254 nm.

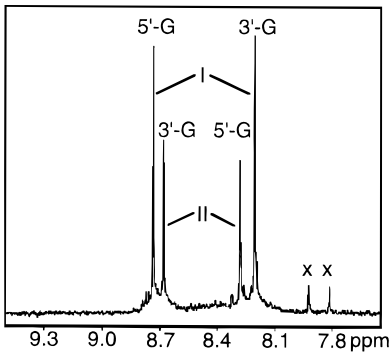

Figure 2. H8 ^{1}H NMR signals of **Bip**Pt(d(GpG)) at pH 3.5, 20 °C (x indicates signals of a third **Bip**Pt(d(GpG)) species mentioned in text).

Results

Treatment of d(GpG) with 1 equiv of [(*R*,*S*,*S*,*R*)-**Bip**Pt$(H_2O)_2]^{2+}$ at pH 3.5 and 20 °C generated two major, spectrally similar products (**I** and **II**) in a 55:45 ratio (reaction time ≤ 30 min). Each product had a pair of H8 ^{1}H NMR signals (Figure 2) with pH-independent shifts, indicating N7 coordination of Pt.[3] The reaction was repeated, using both dilute (0.8 mM) and 0 °C conditions, with similar results, suggesting that the two products are not oligomers. The pH 7 reaction also yielded the same product distribution, indicating that the **Bip** chirality is maintained under these conditions. Heating **Bip**Pt(d(GpG)) at 55 °C resulted in a slight **I**:**II** population redistribution from ~55:45 to ~65:35 after 2 h but no further change up to 24 h. No exchange of magnetization between H8 signals was observed in saturation transfer experiments collected at 45 °C, indicating slow interconversion between **I** and **II**. Thus, **II** is a more favored kinetic product than a thermodynamic product, although **I** is more favored both kinetically and thermodynamically.

The two main adducts, separated by HPLC, showed no appreciable interconversion after 24 h at 25 °C, indicating extremely slow **I**−**II** interconversion. However, the separated products equilibrated slowly at 40 °C to the same ~2:1 mixture; the equilibration rates ($(5.7 \pm 0.4) \times 10^{-5}$ s^{-1} at pH 3 and $(5.9 \pm 0.3) \times 10^{-5}$ s^{-1} at pH 7) are pH independent (Supporting Information). This result demonstrates that the **Bip** configuration, as expected, is the same in **I** and **II** since a change in configuration would require base-catalyzed inversion at one NH, and the rate would be faster at pH 7.

The equilibration in dilute HPLC isolates at moderate temperature demonstrates that **I** and **II** must be conformers or isomers with the same **Bip**Pt:d(GpG) ratio. Both the invariance of the **I**:**II** product formation ratio and the absence of new species on treatment of (*R*,*S*,*S*,*R*)-**Bip**Pt with a 10-fold excess of d(GpG) strongly indicate that the adducts have a 1:1 **Bip**Pt:d(GpG) ratio. The MALDI (Matrix-Assisted Laser Desorption/

(23) Sato, M.; Sato, Y.; Yano, S.; Yoshikawa, S. *J. Chem. Soc., Dalton Trans.* **1985**, 895−898.
(24) Hoffman, R. E.; Davies, D. B. *Magn. Reson. Chem.* **1988**, *26*, 523−525.
(25) Kumar, A.; Ernst, R. R.; Wüthrich, K. *Biochem. Biophys. Res. Commun.* **1980**, *95*, 1−6.
(26) Bodenhausen, G. *Prog. Nucl. Magn. Reson. Spectrosc.* **1981**, *14*, 137−173.
(27) Sklenár, V.; Miyashiro, H.; Zon, G.; Miles, H. T.; Bax, A. *FEBS Lett.* **1986**, *208*, 94−98.
(28) Keller, J.; Clowes, R. T.; Davis, A. L.; Laue, E. D. *Met. Enzymol.* **1994**, *239*, 145−207.
(29) Yao, S.; Plastaras, J. P.; Marzilli, L. G. *Inorg. Chem.* **1994**, *33*, 6061−6077.

Table 1. Assigned Signals (ppm) for BipPt(d(GpG)) at 7 °C, pH 3.5

	G	H8	H1′	H2′	H2″	H3′	H4′	31P
Form **I**	5′	8.76	6.32	2.48	2.73	4.82	4.13	−3.2
	3′	8.22	6.23	2.32[a]	2.37[a]	4.54	4.16	
Form **II**	5′	8.30	6.17	2.76	2.94	4.49	3.97	−2.56
	3′	8.70	6.15	2.35	2.78	4.66	4.46	

[a] No distinction between H2′ and H2″ was possible on the basis of DQF COSY or NOESY data.

Ionization) mass spectrometry data show an ion at *m*/*z* 959 corresponding to a 1:1 **Bip**Pt:d(GpG) ratio (Supporting Information). No ions were observed at higher *m*/*z* values.

Combined 2D NMR experiments allowing ^{1}H (Table 1), ^{13}C, and ^{31}P NMR assignments are detailed in the Supporting Information. Each pair of H8 ^{1}H NMR signals has a large dispersion (Figure 2) and a medium NOESY cross-peak, features consistent with HH conformers.[5−7,12] The H8−H8 distance estimates for forms **I** and **II** were both in the medium distance (2.5−3.5 Å) range, suggesting very similar H8−H8 distances within a range consistent with HH bases. For comparison, H8−H8 distances in HT models of d(GpG) adducts are 5−5.5 Å. No H8−H1′ cross-peaks were observed in the 300 ms mixing time NOESY spectrum, indicating that all of the G's are *anti* since an intense H8−H1′ cross-peak would be observed for a *syn* G. The absence of H8−H1′ NOE cross-peaks has been noted in other systems and interpreted as indicating an *anti* residue.[30,31] However, the absence of these NOEs may also indicate an unusual glycosyl bond orientation in these adducts. Also, shifts of all of the C8 signals were ∼141−142 ppm (Supporting Information), the normal C8 shift range. Downfield-shifted C8 signals have been reported for *syn* bases.[8]

For **I**, the 5′-G H8 signal is downfield and the 3′-G H8 signal upfield (Table 1); this H8 chemical shift relationship is opposite to that found for **II** and for *cis*-Pt(d(GpG))$(NH_3)_2$.[3,4] Strong 5′-G H8−H3′ NOE cross-peaks and the absence of an H1′−H2′ DQF COSY cross-peak[32] indicate that the 5′-G sugars of **I** and **II** have N-puckers. Both the absence of strong 3′-G H8−H3′ NOE cross-peaks for forms **I** and **II** and the pattern of observable DQF COSY cross-peaks indicated that the two forms had a 3′-G S-sugar.

As mentioned above, the HH2 conformer is unprecedented, but the NMR data and consideration of possible cross-linking pathways presented below suggested that the HH2 conformer was the only species that could account for our results. To determine if the proposed HH2 adduct was a feasible cross-linked species, MMD calculations were performed with NMR restraints from forms **I** and **II** on both HH1 and HH2 models (four sets of calculations) since it was not clear from experimental data which form was HH1 or HH2. Two sets of calculations (HH1 with form **I** restraints and HH2 with form **II** restraints) gave computed structures nearly twice as low in energy as those generated with the other combinations. Therefore, we shall associate form **I** with the HH1 conformer and form **II** with the HH2 conformer. Although we shall describe below some of the computed structural data, it should again be emphasized that these calculations were done primarily to determine if the HH2 conformer was energetically feasible. The HH2 model of lowest energy was only ∼1.2 kcal/mol higher in energy than the HH1 model of lowest energy. Moreover,

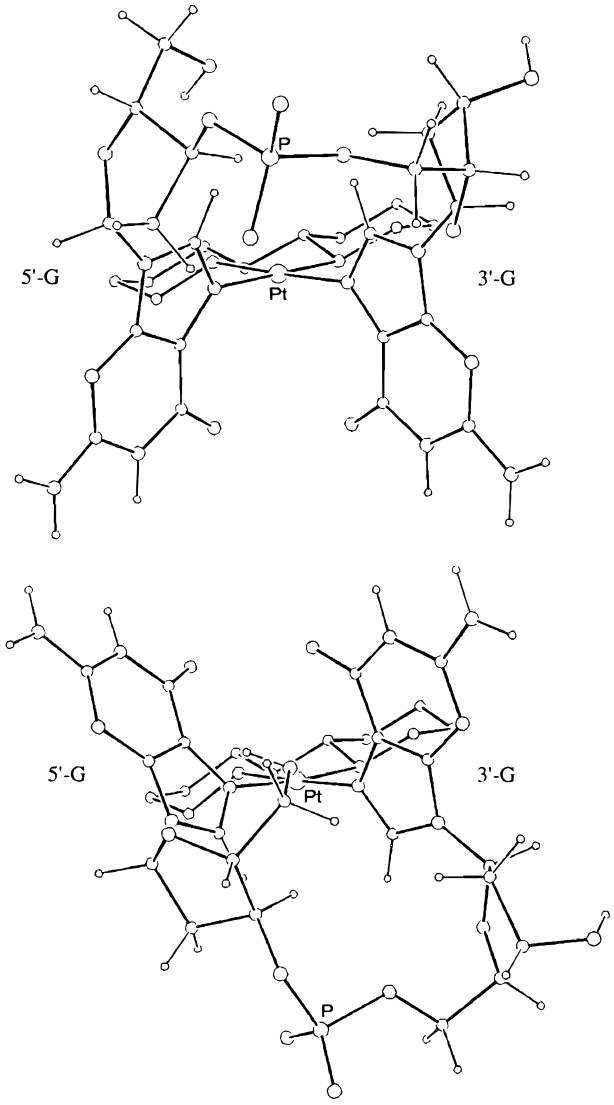

Figure 3. Views of HH1 (top) and HH2 (bottom) models of lowest energy with the **Bip** ligand to the rear. The d(GpG) orientations are analogous to those shown in Figure 1. The **Bip** hydrogens were omitted for clarity.

when no NMR restraints were used in the calculations, the HH2 conformer of lowest energy was actually ∼2 kcal/mol more stable than the HH1 conformer of lowest energy. Thus, our calculations show that the HH1 and HH2 conformers can both be expected to exist in comparable abundance.

We shall emphasize the models from calculations with NMR restraints. Except for the different propagation directions of the phosphodiester backbone, models of the HH1 and HH2 conformers appear to have very similar structures (Figure 3), consistent with the relatively small difference in the chemical shift, NOE, or coupling constant pattern observed for the two forms. The structure of HH2 has no unusual steric or other problems. The H8−H8 distances in the HH1 and HH2 models were 2.9 and 3.2 Å, respectively. In both models, the 5′-G and 3′-G sugar puckers were N and S, respectively. The 5′-G and 3′-G residues were in *anti*, *anti* HH orientations. In accordance with the NMR restraints, the 5′-G glycosyl angles for the HH1 and HH2 models were slightly different, placing 5′-G H8 close to both H2′ and H3′ (∼2.2 Å) in HH2 but close to only H3′ (∼2.6 vs 3.5 Å for H8−H2′) in HH1.

The HH2 model of lowest energy had a 5′-G O6−NH H-bond, which canted the 5′-G H8 into the shielding cone of

(30) Kaspárková, J.; Mellish, K. J.; Qu, Y.; Brabec, V.; Farrell, N. *Biochemistry* **1996**, *35*, 16705−16713.
(31) Patel, D. J.; Kozlowski, S. A.; Nordheim, A.; Rich, A. *Proc. Natl. Acad. Sci. U.S.A.* **1982**, *79*, 1413−1417.
(32) Widmer, H.; Wüthrich, K. *J. Magn. Reson.* **1987**, *74*, 316−336.

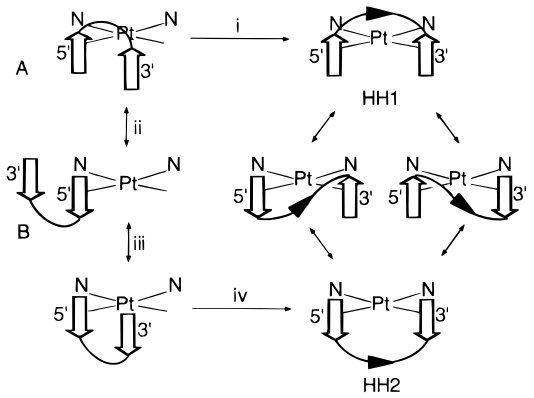

Figure 4. Hypothetical adduct formation pathways for the reaction of d(GpG) with a *cis*-PtA_2 compound. Step i or steps ii + i show chelate formation of the well-recognized HH1 adduct. Step iv or steps iii + iv show formation of the HH2 adduct. Interconversion of the HH1 and HH2 conformers via sequential 180° rotations of the 5′-G and 3′-G bases is shown at the right of the figure.

3′-G. This canting explains the H8 chemical shift relationship observed experimentally for form **II**. The HH1 model places 3′-G O6 close to a **Bip** NH, and a hydrogen bond is indicated by the canting revealed by the 5′-G H8 downfield/3′-G H8 upfield relationship found experimentally and the calculations without NMR restraints. The MMD calculations using no NMR information but using HH conformers with different directions of backbone propagation, as shown in Figure 1, gave essentially the same structures as those computed with NOE restraints.

Discussion

Our results show that **Bip**Pt(d(GpG)) has two major conformers. The most unusual of the two conformers (HH2) has a unique new conformation. Although MMD calculations indicate that it has no unfavorable structural features, the existence of such a conformer has not been predicted in previous studies. The other conformer (HH1) has a conformation similar to that found in previous studies. The rate of interconversion between the HH1 and HH2 forms is slow, and the process probably involves HT intermediates, as seen on the right of Figure 4. A third, consistently observed minor **Bip**Pt(d(GpG)) conformer is probably such an HT conformer. Although too minor for characterization, it has two upfield H8 signals (Figure 2). In related studies in progress with other (**CCC**)Pt systems, we have detected higher percentages of similar adducts having two upfield H8 signals. Preliminary 2D NMR results indicate that these are HT conformers.

For cases in which **Bip**Pt compounds of guanine ligands can be compared directly with similar compounds derived from cisplatin and other Pt analogues, the evidence shows that the same conformers are formed, but dynamic interconversion of these conformers is much slower for the **Bip**Pt compounds.[19,22,33] MMD calculations similar to those described above indicate that the HH2 conformer is possible for the analogue derived from cisplatin, *cis*-Pt(d(GpG))$(NH_3)_2$. In this case, no NMR restraints were available, and the only new input into the HH2 calculations was the change in the direction of propagation of the backbone. However, the d(GpG) moiety in the HH2 conformer of *cis*-Pt(d(GpG))$(NH_3)_2$ gave all the features observed in the HH2 conformer of **Bip**Pt(d(GpG)). These include the sugar puckers, glycosyl bond orientations, etc. We believe interconverting conformers exist but would be undetectable by NMR spectroscopy for the more fluxional *cis*-Pt(d(GpG))$(NH_3)_2$. Furthermore, the study of the **Bip**Pt(d(GpG)) adduct has an advantage over the study of such fluxional *cis*-Pt(d(GpG))A_2 adducts in evaluating adduct formation from reactants. The **Bip**Pt(d(GpG)) HH2 conformer was observed at a slightly greater abundance than at equilibrium; thus, it must be formed directly from reactants. An analysis of how the HH2 conformer can be produced directly is instructive in understanding the structural differences between HH1 and HH2.

We propose likely but hypothetical cross-linking pathways consistent with the fundamental chemistry of Pt-G adducts depicted on the left of Figure 4. Critical points to appreciate are that the Pt must initially bind to either the 3′-G or the 5′-G[34] and that once the first bond is made between Pt and the first G, any symmetry of the reactive Pt center is eliminated. For simplicity, the figure shows only the case in which 5′-G binds first; a similar scheme would result for 3′-G binding (Supporting Information). Initial binding of the 5′-G orients the 3′-G next to or away from the empty Pt coordination position (A and B in Figure 4). In the latter instance (B), the 3′-G cannot bind until some movement occurs. If rotation about the N7 bond is fast compared to the glycosyl bond rotation, the well-known HH1 conformer is formed via steps ii and i (Figure 4). However, if glycosyl bond rotation is fast compared to Pt−N7 bond rotation, cross-linking produces HH2 via steps iii and iv (Figure 4). These pathways are reasonable for cisplatin and any of its typical analogues; in such cases, however, the evidence discussed below suggests that the kinetic product is too dynamic to be observed.

BipPt(d(GpG)) form **I** is unusual in having spectral features very similar to those of the d(GpG) *cis*-Pt$(NH_3)_2$ cross-link within duplexes, where the HH1 conformation is better defined. In particular, the typical H8 shift relationship in a duplex is 5′-G H8 downfield and 3′-G H8 upfield,[9,10,13,14] and the ^{31}P shift is well defined at ca. −3.2 ppm.[9,13,35−37] Also, the 5′-G H8 shift of form **I** is very close to this shift for most duplexes, ∼8.7 ppm.[9,10,13,14] HH1 cross-links usually have one base canted toward the other,[4−7,12,38] and the H8 of the more canted base is upfield due to the ring-current effects of the less canted base.[11] Depending on which base is canted, opposite shift relationships are found for the 3′-G H8 and 5′-G H8 signals. The 3′-G H8 signal is always upfield in duplexes, indicating that the 3′-G base is canted. Both types of canting are observed in the crystal structure of the single-stranded species, *cis*-Pt(d(pGpG))$(NH_3)_2$, which has four independent molecules, all with the HH1 conformation.[39,40] In solution, only upfield 5′-G H8/downfield 3′-G H8 shifts have been detected for single-stranded species except in two reported cases.[41,42] It is of considerable interest that **Bip**Pt(d(GpG)) form **I** is a third exception. The opposite

(33) Ano, S. O.; Intini, F. P.; Natile, G.; Marzilli, L. G., manuscript in preparation.

(34) Gonnet, F.; Reeder, F.; Kozelka, J.; Chottard, J.-C. *Inorg. Chem.* **1996**, *35*, 1653−1658.
(35) den Hartog, J. H. J.; Altona, C.; van Boom, J. H.; van der Marel, G. A.; Haasnoot, C. A. G.; Reedijk, J. *J. Am. Chem. Soc.* **1984**, *106*, 1528−1530.
(36) Wilson, W. D.; Heyl, B. L.; Reddy, R.; Marzilli, L. G. *Inorg. Chem.* **1982**, *21*, 2527−2528.
(37) Marzilli, L. G.; Reily, M. D.; Heyl, B. L.; McMurray, C. T.; Wilson, W. D. *FEBS Lett.* **1984**, *176*, 389−392.
(38) Berners-Price, S. J.; Ranford, J. D.; Sadler, P. J. *Inorg. Chem.* **1994**, *33*, 5842−5846.
(39) Sherman, S. E.; Gibson, D.; Wang, A. H.-J.; Lippard, S. J. *Science* **1985**, *230*, 412−417.
(40) Sherman, S. E.; Gibson, D.; Wang, A. H. J.; Lippard, S. J. *J. Am. Chem. Soc.* **1988**, *110*, 7368−7381.
(41) Dunham, S. U.; Lippard, S. J. *J. Am. Chem. Soc.* **1995**, *117*, 10702−10712.
(42) Hambley, T. W.; Ling, E. C. H.; Messerle, B. A. *Inorg. Chem.* **1996**, *35*, 4663−4668.

shift relationship for **I** and **II** is consistent with a difference involving which base is most canted.

In contrast to the well-defined, relatively narrow shift ranges for duplexes, single-stranded species have very variable H8 shifts, with the 5′-G H8 signal found from ∼8.0 to ∼9.0 ppm and the 3′-G H8 shift from ∼8.5 to ∼9.5 ppm in the various species.[3−7,12,38] The broad range of H8 shifts for single-stranded species is just one piece of evidence for dynamic exchange between multiple single-stranded conformers. Since the HH2 conformer has not been foreseen in the literature and HT conformers were considered to be unlikely, the only dynamic process that has been discussed at any length is the change in base canting of the HH1 conformer. Our results raise the possibility that there was also some population of HH2 and HT conformers in these single-stranded species. This possibility gains support from the broadness of the range of ^{31}P NMR shifts reported for the single-stranded species, including values close to that for form **II**.[5,9,35] Additional support for the possibility can be found in the very large ∼7.8 to 8.8 ppm ranges of H8 shifts for both 3′- and 5′-G's defined by the three observed conformers of **Bip**Pt(d(GpG)).

Mixtures of several conformers also explain the many failures to obtain a crystal structure of *cis*-Pt(d(GpG))$(NH_3)_2$. The first crystallographic success (with *cis*-Pt(d(pGpG))$(NH_3)_2$)[39,40] revealed that it had the accepted HH1 conformation; this finding apparently confirmed the NMR interpretation. However, the crystal structure also revealed a stabilizing hydrogen bond between the 5′-phosphate group and the *cis* NH_3.[39,40] Our modeling studies with *cis*-Pt(d(pGpG))$(NH_3)_2$ also give HH1 conformers with this hydrogen bond. The HH1 conformer is slightly more stable than the new HH2 conformer, which lacks this hydrogen bond.

In conclusion, our results in this first report of a second *anti*, *anti* HH d(GpG) conformer place an entirely different perspective on the possible conformers of *cis*-Pt(d(GpG))$(NH_3)_2$ and larger single-stranded species in solution. The new HH and HT conformers most probably exist as part of a dynamic mixture. Such a mixture could explain the relatively rapid G N(1)H proton exchange with solvent H_2O observed for cross-links in duplexes since HT or HH2 conformers would have one and two bases, respectively, exposed to solvent. The HH1 conformer found in duplexes at low temperatures is probably still the predominant form at 37 °C. However, minor HT or HH2 conformers in duplexes could have a role in recognition by repair enzymes or by damage recognition proteins.

Acknowledgment. This work was supported by NIH Grant GM 29222 (to L.G.M.) and NATO CRG. 950376 (to L.G.M. and G.N.) as well as MURST (Contribution 40%), CNR, and EC (COST Chemistry project D8/0012/97 (to G.N.)). NSF Grant ASC-9527186 supported the use of the Internet for remote collaborative research. We thank the Emory Microchemical Facility for MALDI-MS.

Supporting Information Available: Figures showing HPLC separation of the conformers, rate constant graphs, MALDI mass spectrometry data; detailed 2D NMR assignment procedures and partial 2D NMR spectra; stereoviews of molecular modeling structures; and additional cross-linking pathways (11 pages, print/PDF). See any current masthead page for ordering information and Web access instructions.

JA9805674